

LaViPlan : Language-Guided Visual Path Planning with RLVR

Hayeon Oh
ETRI

oph516@etri.re.kr

Abstract

*Out-of-distribution (OOD) scenarios in autonomous driving refer to situations that deviate from the training domain, often leading to unexpected and potentially hazardous behavior from planners that lack prior exposure to such cases. Recently, Vision-Language Models (VLMs) have been introduced into autonomous driving research for their promising generalization capabilities in OOD settings. Early studies demonstrated that VLMs could recognize OOD scenarios and generate user-level decisions such as “go straight” or “turn right.” However, a new challenge has emerged due to the misalignment between the VLM’s high-level decisions or visual reasoning expressed in language, and the low-level predicted trajectories interpreted as actions. In this paper, we propose **LaViPlan**, a framework that leverages Reinforcement Learning with Verifiable Rewards (RLVR) to optimize VLMs using planning-oriented metrics. This approach addresses the vision-language-action misalignment observed in existing VLMs fine-tuned via supervised learning, which can recognize driving scenarios but often produce context-unaware decisions. Experimental results demonstrate that our method improves situational awareness and decision-making under OOD conditions, highlighting its potential to mitigate the misalignment issue. This work introduces a promising post-training paradigm for VLM agents in the context of autonomous driving.*

1. Introduction

Out-of-distribution (OOD) scenarios in autonomous driving refer to rare or novel situations that deviate from the training domain, often leading to unexpected and unsafe behavior by learned planning policies. These scenarios pose critical challenges, particularly when the planner fails to generalize beyond its supervised experience. To address this, recent research has explored the integration of Vision-Language Models (VLMs) [1, 4, 15] into autonomous driving. VLMs have demonstrated strong generalization capabilities across diverse tasks and modalities, making them a promising ap-

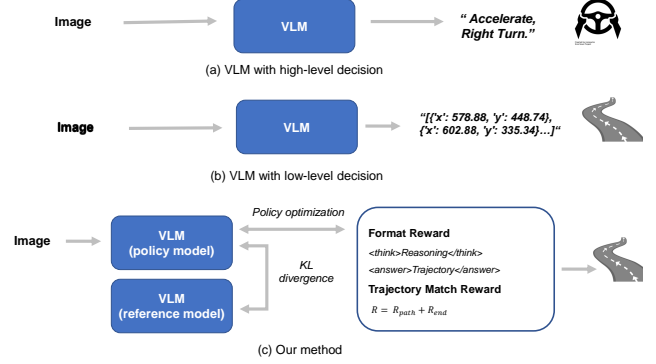


Figure 1. (a) VLMs generating high-level commands (e.g., “Accelerate, Right Turn”) based on scene understanding, but lacking direct trajectory grounding. (b) VLMs producing low-level outputs such as trajectories without explicit reasoning, often leading to semantically inconsistent or context-unaware behavior. (c) Our proposed method introduces a differentiable connection between vision-language reasoning and action space using RLVR. The reward consists of a format-based reasoning verification and trajectory alignment, optimized under KL regularization between the policy and reference model.

proach for handling OOD scenarios. Early research showed that VLMs could identify anomalous or unseen driving contexts and generate high-level user-aligned decisions (e.g., “go straight,” “turn right”) [10, 11]. However, while VLMs can recognize and describe OOD scenes, their final decisions—especially in the form of predicted trajectories—can often be misaligned with the visual reasoning they produce. This issue reflects a broader challenge in aligning language-based reasoning with action-level planning, which we refer to as the vision-language-action misalignment. In this paper, we propose to address the misalignment by leveraging Reinforcement Learning with Verifiable Rewards (RLVR), guided by planning-oriented metrics. Our method aims to steer VLMs toward context-aware decision-making that is consistent with their situational reasoning. Our key contributions are summarized as follows:

- We propose a reinforcement learning framework that explicitly optimizes planning-oriented metrics in VLMs.

Our method demonstrates a step toward aligning language-guided reasoning with action-oriented tasks in autonomous driving.

- Through both quantitative and qualitative analyses, we reveal that RLVR shifts the model’s generation from linguistically faithful outputs to functionally accurate trajectories, indicating a trade-off between semantic similarity and task-specific reasoning.
- Experimental results demonstrate that RLVR requires significantly fewer training samples compared to supervised fine-tuning while still achieving performance gains, showing that including hard cases during RL yields better generalization.

2. Related Works

2.1. Vision and Language Foundation Models

End-to-end autonomous driving has recently gained attention due to its simplicity and efficiency, as well as its ability to address the suboptimality issues that arise from misaligned objectives between modular components. This paradigm reduces information loss and computational overhead by eliminating intermediate representations. However, the visual abstraction in end-to-end systems often simplifies complex scene information, which can result in the loss of critical cues. Furthermore, achieving generalization across diverse driving scenarios remains challenging. Simply increasing the scale of training data is not always feasible, particularly in long-tail or out-of-distribution (OOD) scenarios where labeled data is limited or sparse. To overcome these challenges, recent studies have explored integrating Vision-Language Models (VLMs) into autonomous driving, as VLMs are capable of grounding and reasoning about previously unseen situations through their multi-modal understanding. These models typically combine pre-trained large language models (LLMs) with visual encoders, where driving instructions or ego vehicle states are provided as textual input to the LLM, and single- or multi-view images are passed through the visual encoder [10, 12, 19, 22, 23, 25, 30, 31]. More recent research has extended these models with techniques such as 3D perceptual positional embeddings [6, 27, 34] and counterfactual learning [20, 27] to enable context-aware decision-making in complex environments.

2.2. Reinforcement Learning for Language Models

Reinforcement Learning from Human Feedback (RLHF) has demonstrated the effectiveness of aligning VLMs with human preferences with Proximal Policy Optimization (PPO) [13]. However, RLHF has computational overhead due to the multiple components, including a reference model, reward model, critic, and a newly trained generative model. Additionally, the reliance on human annotators

further increases the cost of training. In contrast, Group Relative Policy Optimization (GRPO) [8] enhances the reasoning and arithmetic capabilities of VLMs by learning directly from comparisons between the policy model and the reference model, without requiring an explicit reward model or critic. The authors advocate for a rule-based reward model, arguing that neural reward models may be vulnerable to reward hacking during large-scale reinforcement learning. Reinforcement fine-tuning with RLVR has recently been applied to tasks such as object detection, classification [16], mathematics [5], and code generation, where ground-truth outputs are either unambiguous or can be verified through test cases. It has also been extended to robotics domains, including manipulator control [24, 28] and autonomous driving [11, 18], where the correctness of the output can be evaluated through physical simulations or pre-defined behavioral criteria. The objective nature of these tasks makes the design and validation of reward signals relatively straightforward. The effectiveness of GRPO has also been theoretically analyzed: recent work shows that GRPO improves the success rate of reward-maximizing outputs through a fixed-point dynamic process and provides guarantees on preference amplification over the reference model [17]. Furthermore, its alignment mechanism differs fundamentally from RLHF’s logarithmic pooling, instead applying nonlinear transformations that prioritize relatively more rewarding outputs under group-based comparisons [26]. In this work, we explore the use of Multimodal Large Language Models (MLLMs) for autonomous driving by leveraging RLVR with planning-oriented metrics, such as Average Displacement Error (ADE) and Final Displacement Error (FDE). Our approach aims to fine-tune MLLMs through objective and verifiable reward signals, demonstrating the effectiveness of RLVR in planning-centric tasks such as trajectory prediction in autonomous driving.

3. Methodology

3.1. Preliminary

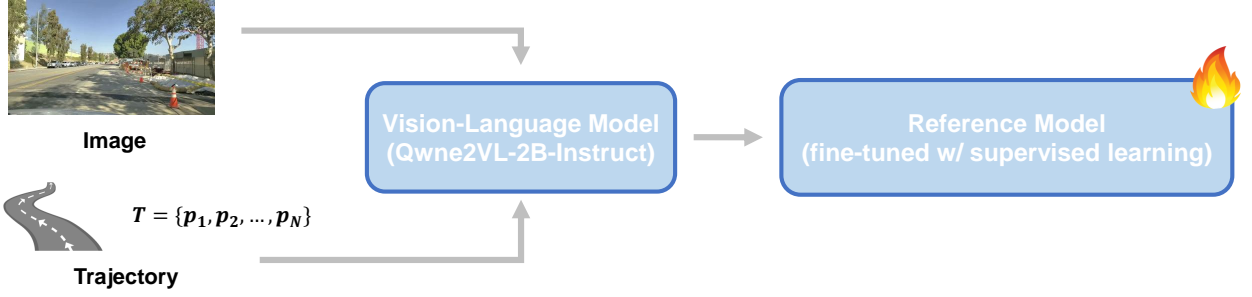
Reinforcement Learning from Verifier Rewards RLVR aims to optimize a policy π_θ by maximizing the expected reward from a verifier while maintaining proximity to a reference policy π_{ref} to prevent over-optimization. The objective function is formulated as:

$$\max_{\pi_\theta} \mathbb{E}_{o \sim \pi_\theta(q)} [R_{\text{RLVR}}(q, o)] \quad (1)$$

$$= [R(q, o) - \beta \text{KL}(\pi_\theta(o | q) \parallel \pi_{\text{ref}}(o | q))] \quad (2)$$

where q represents the input query, o denotes the generated output, $R(q, o)$ is the reward function provided by the verifier, and β is a regularization coefficient that controls the trade-off between reward maximization and KL divergence

(a) Phase 1 : Supervised Fine-Tuning



(b) Phase 2 : Reinforcement Fine-Tuning with Verifiable Reward

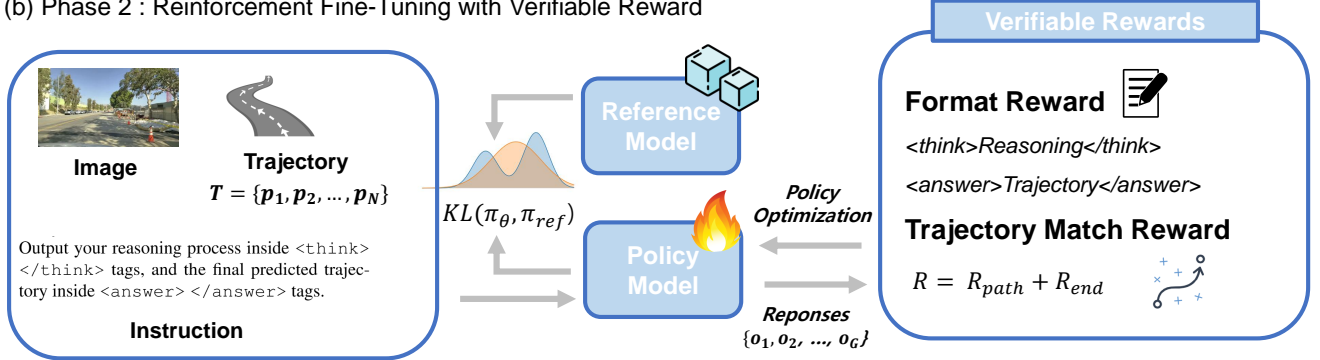


Figure 2. Overview of proposed method. (a) In Phase 1, the Vision-Language Model is fine-tuned with supervised learning using paired image-instruction-trajectory data. (b) In Phase 2, reinforcement fine-tuning with verifiable rewards based on format accuracy of responses and trajectory alignment. The policy model is optimized via KL divergence from a supervised reference model with group size of G .

penalty. The KL divergence term ensures that the learned policy does not deviate significantly from the reference policy, maintaining stability during training.

Group Relative Policy Optimization GRPO extends the Proximal Policy Optimization (PPO)[21] by incorporating group-relative advantage estimation. The advantage function is computed using group statistics to reduce variance:

$$\hat{A}_{i,t} = \frac{R_i - \text{mean}(\{R_i\}_{i=1}^G)}{\text{std}(\{R_i\}_{i=1}^G)} \quad (3)$$

where G represents the group size, R_i is the reward for the i -th response, and the advantage $\hat{A}_{i,t}$ is normalized using the mean and standard deviation of rewards within the group. This normalization helps stabilize training by reducing the impact of reward scale variations.

The GRPO objective function combines the clipped surrogate objective from PPO with the group-relative advantages:

$$\mathcal{J}_{GRPO} = \frac{1}{G} \sum_{i=1}^G \frac{1}{|o_i|} \sum_{t=1}^{|o_i|} \left[\min \left\{ \frac{\pi_{\theta}(o_{i,t}|q, o_{i,<t})}{\pi_{\theta_{\text{old}}}(o_{i,t}|q, o_{i,<t})} \hat{A}_{i,t}, \right. \right. \\ \left. \left. \text{clip} \left(\frac{\pi_{\theta}(o_{i,t}|q, o_{i,<t})}{\pi_{\theta_{\text{old}}}(o_{i,t}|q, o_{i,<t})}, 1 - \varepsilon, 1 + \varepsilon \right) \hat{A}_{i,t} \right\} \right. \\ \left. - \beta \text{KL}[\pi_{\theta} \parallel \pi_{\text{ref}}] \right] \quad (4)$$

where $\pi_{\theta_{\text{old}}}$ represents the policy from the previous iteration, $|o_i|$ is the length of the i -th output response, ε is the clipping parameter, and the min operation implements the conservative policy update mechanism characteristic of PPO. The KL divergence term provides additional regularization to maintain training stability.

3.2. RLVR with Planning-Oriented Metrics

In this work, we apply GRPO to autonomous driving by designing a reward function that directly reflects planning performance as shown in Fig. 2. Specifically, we define the reward using commonly adopted trajectory evaluation metrics: Average Displacement Error (ADE) and Final Displacement Error (FDE).

$$R_{\text{planning}} = -\log \left(1 + \frac{1}{N} \sum_{i=1}^N \|\hat{p}_i - p_i\|_2 \right) - \log (1 + \|\hat{p}_N - p_N\|_2) \quad (5)$$

The first term encourages the predicted trajectory $\hat{T} = \{\hat{p}_1, \hat{p}_2, \dots, \hat{p}_N\}$, where each $\hat{p}_i \in \mathbb{R}^2$ represents an (x, y) position in image plane to stay close to the ground-truth trajectory $T = \{p_1, p_2, \dots, p_N\}$, where each $p_i \in \mathbb{R}^2$ over the full horizon (ADE), while the second term penalizes deviations at the final timestep (FDE). We apply logarithmic smoothing for numerical stability and better learning dynamics. In addition to planning accuracy, we incorporate a formatting reward R_{format} , which encourages adherence to the expected output format with reasoning and response.

$$R = R_{\text{format}} + R_{\text{planning}} \quad (6)$$

4. Experiment

In-Domain Dataset. The ROADWork dataset [7] serves as an OOD benchmark focused on road construction scenarios. Among the entire dataset, 5,430 samples contain image, scene description, and a list of trajectories in image plane. To demonstrate that reinforcement fine-tuning can yield performance improvements even with data less than supervised fine-tuning, we divided the dataset into two subsets: 4,344 samples for supervised fine-tuning and 1,086 samples (20% of full samples) for reinforcement fine-tuning. Training details for supervised fine-tuning and reinforcement fine-tuning can be seen in the Appendix A.

Subsets Defined by Trajectory Variance. We split the dataset into two subsets based on the variance of x-coordinates in the trajectory. One subset comprises trajectories with low lateral variance representing straight trajectory (**Easy**). In contrast, the other subset comprises trajectories with higher lateral variance and more curved trajectories involving left and right turns (**Hard**). Details of the dataset splitting procedure are provided in the Appendix B.

Out-Domain Dataset. The CODA-LM [2] extends the CODA dataset [14] which includes various corner cases such as road construction and adverse weather conditions by augmenting it with natural language captions. The generalization ability of our method under OOD conditions was qualitatively assessed using the corner-case dataset not limited to construction zones.

Dataset and Prompt Design for Reinforcement Fine-Tuning. The dataset for reinforcement fine-tuning

consists of a reasoning description enclosed within `<think></think>` tags, which includes visual reasoning process from the image, and a predicted trajectory represented as a list of 20 (x, y) image coordinates enclosed within `<answer></answer>` tags as shown in Tab. 1. Specifically, the `<think></think>` section provides the rationale behind the prediction, while the `<answer></answer>` section contains the autonomous vehicle’s future trajectory as a sequence of coordinate pairs.

Table 1. Instruction for reinforcement fine-tuning and example of response.

Trajectory Prediction Prompt: Given only the image, predict the autonomous vehicle’s future trajectory as a list of 20 (x, y) image coordinates. You must output your reasoning process inside `<think> </think>` tags, and the final predicted trajectory inside `<answer> </answer>` tags. Strictly follow the output format below: `<think> Reasoning based on visual cues in the image. </think>`
`<answer>[{‘x’: x1, ‘y’: y1}, ..., {‘x’: x20, ‘y’: y20}]</answer>`

Example of Response: `<think>tubular markers on right side of road. work vehicle on right side of road. worker on right sidewalk.</think><answer>[{‘x’: 578.88, ‘y’: 448.74}, {‘x’: 578.56, ‘y’: 442.6}, ..., {‘x’: 602.88, ‘y’: 335.34}]</answer>`

4.1. Experimental Results

4.1.1. Evaluation Results

Tab. 2 shows overall result across multiple foundation models: baseline, supervised fine-tuning, and our proposed method. They are evaluated with ADE and FDE on both easy and hard subsets. In the baseline, VLMs without additional task-specific supervision lack the capability to generalize directly to trajectory planning. In contrast, supervised fine-tuning improves performance and our proposed method achieves the best performance across all metrics. Compared to supervised fine-tuning models, LaViPlan further reduces the errors. This demonstrates the effectiveness of reward optimization in refining planning-oriented outputs beyond what can be achieved with standard supervised

Table 2. Comparison of model performance on ROADWork dataset. ADE and FDE are presented as percentages by normalizing with image resolution for better readability. The models with supervised fine-tuning were trained on the full dataset of 5K samples, while LaViPlan was fine-tuned with 4K samples for supervised learning and an additional 1K samples for reinforcement fine-tuning. **Bolded** values indicate the best performance.

	ADE ↓		FDE ↓	
	Easy	Hard	Easy	Hard
<i>Baseline</i>				
Qwen2VL-2B	52.44	52.77	102.39	105.05
Qwen2VL-7B	60.73	60.71	66.61	67.57
LLaMA3.2-11B	59.27	58.88	74.16	71.44
<i>Supervised Fine-tuning</i>				
Qwen2VL-2B	4.52	5.66	4.46	6.46
Qwen2VL-7B	4.80	6.04	5.08	7.35
LLaMA3.2-Vision-11B	4.52	5.46	5.20	7.10
<i>Reinforcement Fine-tuning</i>				
LaViPlan (ours)	3.62	4.83	3.85	6.09

learning. In summary, these results indicate that (1) VLMs are insufficient for planning tasks without supervised fine-tuning, (2) supervised fine-tuning is essential for grounding planning behaviors, and (3) RLVR with planning-oriented metrics leads to further performance gains by explicitly optimizing for planning.

4.1.2. From Linguistic Consistency to Functional Reasoning.

Table 3. Comparison of Scene Understanding. SFT refers to supervised fine-tuning and RFT refers to reinforcement fine-tuning

	SFT	RFT	Change
BERTScore	0.748	0.712	-4.81%
Entailment (%)	44.8	37.7	-15.85%
Neutral (%)	25.3	29.1	+15.02%
Contradiction (%)	29.9	33.1	+10.70%

We evaluate the linguistic effects of our method on the combined easy and hard subsets using BERTScore [33] and Natural Language Inference (NLI) [3], as shown in Tab. 3. Compared to supervised fine-tuning (SFT), reinforcement fine-tuning (RFT) leads to a decrease in BERTScore, as well as a reduction in entailment and an increase in neutral and contradiction labels. While these results indicate a divergence from ground-truth human-written descriptions, they do not necessarily imply degraded reasoning ability. Rather, we observe a meaningful shift in the model’s reasoning style. As shown in Fig. 3, scene descriptions from RFT tend to be more concise and hazard-focused emphasis-

ing critical elements such as barriers, cones, and work vehicles in terms of planning. In contrast, SFT tends to replicate verbose and linguistically rich but often functionally redundant information. In several scenarios, RFT omits less relevant descriptors (e.g., sidewalks or drum lines) in favor of spatial cues that better support trajectory-level decisions. This trade-off suggests that conventional language metrics may underrepresent reasoning utility in autonomous driving contexts. Despite lower alignment with human-like phrasing, RFT yields improved planning performance, indicating that more effective and actionable reasoning can emerge even as linguistic similarity declines. We advocate for a shift toward task-aware evaluation of vision-language models in safety-critical domains, where functional relevance should take precedence over semantic mimicry.

4.1.3. Evaluating Out-of-Distribution Generalization.

We qualitatively evaluate the proposed method on CODA-LM [2], a zero-shot dataset composed of diverse corner cases involving out-of-distribution (OOD) road hazards. Since CODA-LM does not provide ground-truth trajectories, we rely on visual inspection of the predicted paths to assess plausibility, safety, and contextual awareness. As shown in Fig. 4, the model fine-tuned with RLVR produces more realistic and contextually appropriate trajectories compared to the one trained via supervised fine-tuning. In scenarios involving roadwork, blocked lanes, and ambiguous path constraints, the supervised model often generates overly linear or risk-prone trajectories that lack appropriate deviation or caution. In contrast, the proposed method consistently generates smoother, safer, and more context-aware trajectories, often adjusting path curvature to avoid obstacles such as cones, barriers, and vehicles. These results demonstrate the model’s capacity to generalize to previously unseen situations by aligning its reasoning and path generation with latent planning cues in the scene, even without explicit supervision. While the absence of quantitative metrics in CODA-LM limits numerical evaluation, these qualitative outcomes suggest that reinforcement fine-tuning enhances the model’s ability to adapt to novel driving contexts.

4.2. Ablation Studies

4.2.1. Supervised vs. Reinforcement Fine-Tuning

We analyze the impact of reinforcement fine-tuning by comparing models with and without reinforcement-based optimization. The observed gains over supervised fine-tuning, as reported in Tab. 4, indicate that the reinforcement fine-tuning captures complementary learning signals beyond supervised losses. Interestingly, the effect size varies with task complexity, implying that the reinforcement fine-tuning provides stronger gradient signals in low-uncertainty regimes while remaining effective under harder conditions.



Figure 3. Qualitative comparison of scene reasoning between the SFT (top) and RFT (bottom) models across six scenarios in [7]. While SFT tends to produce more verbose, human-like descriptions that closely resemble natural annotations, the RFT model emphasizes core, task-relevant elements such as cones, barriers, and work vehicles. This shift in reasoning reflects a transition from linguistic fidelity to planning-oriented abstraction, enabling the model to better prioritize hazards and navigable space—even at the cost of similarity to ground-truth descriptions.

Table 4. Impact of Reinforcement Fine-Tuning (RFT) on performance after Supervised Fine-Tuning (SFT), showing consistent improvements across easy and hard scenarios.

	ADE ↓		FDE ↓	
	Easy	Hard	Easy	Hard
Baseline	52.44	52.77	102.39	105.05
SFT	4.52	5.66	4.46	6.46
LaViPlan	3.62	4.83	3.85	6.09
Δ	-19.91%	-14.67%	-13.69%	-5.73%

4.2.2. Effective Sample Set for GRPO

Table 5. Performance impact of different easy-to-hard data ratios when the total number of training samples is held constant.

Ratio	ADE ↓		FDE ↓	
	Easy	Hard	Easy	Hard
9:1	3.84 (-15.0%)	5.05 (+10.7%)	4.09 (-8.3%)	6.31 (-2.3%)
7:3	5.55 (+22.8%)	6.70 (+18.4%)	4.05 (-9.2%)	6.16 (-4.6%)
6:4	3.62 (-19.9%)	4.83 (-14.7%)	3.85 (-13.7%)	6.09 (-5.7%)

To evaluate the impact of sample difficulty on reinforce-

ment fine-tuning, we fix the SFT:RFT ratio at 4:1 (corresponding to 4,344 and 1,086 samples, respectively), and vary the proportion of easy and hard samples within this fixed budget. As shown in Tab. 5, allocating a larger portion of hard scenarios (up to 40%) leads to consistent improvements across both ADE and FDE, particularly for hard cases. These results suggest that the reinforcement fine-tuning benefits from challenging samples that provide richer learning signals, helping the model generalize better in complex planning situations.

4.2.3. Impact of Reasoning in Two-Phased Fine-tuning

We ablate the use of explicit reasoning in both supervised fine-tuning (phase 1) and subsequent reinforcement fine-tuning (phase 2) to investigate its effect, as shown in Tab. 6 and Tab. 7.

Reasoning Impact on Supervised Fine-Tuning. In supervised fine-tuning (phase 1), models trained with reasoning outperformed those without, although the margin was relatively small. Both versions achieved significant gains over the instruction-tuned baseline, with over 90% reductions in ADE and FDE across all subsets. This indicates that supervised fine-tuning plays a major role in grounding planning behavior, and the addition of reasoning further enhances the model’s ability to contextualize scenes.



Figure 4. Qualitative results comparing supervised fine-tuning (top) and RLVR-based reinforcement fine-tuning (bottom) across diverse out-of-distribution (OOD) hazard scenarios. Examples include construction zones, adverse weather (e.g., rain and poor lighting), unexpected pedestrian behavior, and road obstacles. The proposed method generates more accurate and context-aware trajectories under complex conditions, indicating better robustness in real-world hazard cases.

Table 6. Ablation Study: Effect of Reasoning on Supervised Fine-Tuning (phase 1).

	ADE ↓		FDE ↓	
	Easy	Hard	Easy	Hard
Baseline	52.44	52.77	102.39	105.05
w/o reasoning	4.14 (-92.10%)	5.46 (-89.66%)	4.40 (-95.70%)	6.65 (-93.67%)
w/ reasoning	4.12 (-92.14%)	5.31 (-89.94%)	4.44 (-95.66%)	6.51 (-93.80%)

Reasoning Impact on Reinforcement Fine-Tuning. In reinforcement fine-tuning (phase 2), where reinforcement

Table 7. Ablation Study: Effect of Reasoning on Reinforcement Fine-Tuning (phase 2).

	ADE ↓		FDE ↓	
	Easy	Hard	Easy	Hard
Baseline	4.52	5.66	4.46	6.46
w/o reasoning	3.71 (-17.7%)	4.95 (-12.6%)	3.96 (-11.2%)	6.26 (-3.1%)
w/ reasoning	3.62 (-19.9%)	4.83 (-14.7%)	3.85 (-13.7%)	6.09 (-5.7%)

fine-tuning is applied on top of the already fine-tuned models from phase 1, the inclusion of reasoning continues to offer additional benefits. Although the overall improvements

are more modest than those observed in phase 1, models with reasoning consistently outperform those without across both ADE and FDE. The performance gap is slightly larger in the hard subset, suggesting that reasoning becomes more useful in complex scenarios. These findings imply that explicit reasoning, when preserved throughout both fine-tuning stages, provides stable gains by promoting structured understanding aligned with planning objectives.

5. Discussion and Limitations

We proposed LaViPlan, a reinforcement learning framework guided by planning-oriented metrics, as a method for fine-tuning VLMs on autonomous driving tasks. Our findings suggest that RLVR not only enhances the zero-shot scene understanding capabilities of LLM agents but also shows potential in mitigating the misalignment between vision, language, and action. In conclusion, several limitations remain and highlight directions for future research. (1) The planning reward is sparse, as it is only obtained after the entire rollout, which highlights the need for step-wise feedback during policy optimization. This may have constrained the potential of GRPO, limiting the effectiveness of intermediate decision-making signals [32]. (2) While the improvements in planning performance indicate progress, they are not sufficient to claim complete resolution of vision-language-action misalignment. A more context-aware evaluation metric is needed to assess whether model decisions are grounded with context-awareness [29]. (3) The extent to which this effectiveness transfers to world models remains an open question—particularly in the realm of counterfactual reasoning over out-of-distribution (OOD) actions encountered in sequential decision-making tasks.

Appendix

A. Training Details

Table 8. Hyperparameters for language world model training.

Hyperparameter		
SFT	Global Batch size	128
	Batch size per GPU	4
	LoRA rank [9]	64
	LoRA α	16
	Epoch	1
	Learning rate	1×10^{-5}
	Weight decay	0.1
RLVR	Max response length	1024
	Batch size	128
	PPO (GRPO) mini batch size	4
	KL loss coefficient	0.04
	Group size	4
	Learning rate	5×10^{-6}
Sampling	Top- p	0.95
	Temperature	1.2
	Repetition Penalty	1.2

Through an empirical study, we observed that for effective policy model optimization using the GRPO algorithm [8], the responses of the reference model must exhibit sufficient diversity within a limited group size. Accordingly, we increased the repetition penalty and temperature slightly compared to the default settings.

B. Split Dataset

B.1. Dataset Construction and Splitting Strategy

To enable both supervised and reinforcement fine-tuning for visual path planning, we split the dataset into Supervised Fine-Tuning (SFT) and Reinforcement Fine-Tuning (RFT) subsets using a structured and variance-aware strategy. We first load the complete set of trajectory metadata D and determine the target ratios for SFT versus RFT (e.g., 4:1), as well as the distribution of turning and straight trajectories within each subset (e.g., 6:4 or 4:6 depending on the setting). For each trajectory $d \in D$, we calculate the variance of its x -coordinates, which serves as a proxy for trajectory curvature. We then sort the trajectories in descending order of x -variance. Based on this ordering, we classify the top- N trajectories with high variance as turning trajectories and the remaining as straight trajectories. From these, we allocate subsets to SFT and RFT splits: a portion of turning trajectories to RFT-turn and the remainder to SFT-turn, and similarly, straight trajectories to SFT-straight and RFT-straight.

Algorithm 1 Splitting Dataset into SFT and RFT data for Visual Path Planning

- 1: Load entire trajectory metadata list D
- 2: Compute desired split sizes for:
 - SFT vs. RFT (e.g., 4:1 ratio)
 - Straight vs. Turn trajectories (e.g., 6:4 or 4:6 depending on SFT/RFT)
- 3: For each sample $d \in D$, compute variance of x -coordinates over its trajectory
- 4: Sort all samples in descending order of x -variance
- 5: Split into two groups:
 - Top- N samples with high variance \rightarrow turning samples
 - Remaining samples \rightarrow straight samples
- 6: From turning samples:
 - Assign the first N_1 to RFT-turn
 - Assign the remaining N_2 to SFT-turn
- 7: From straight samples:
 - Assign first M_1 to SFT-straight
 - Assign next M_2 to RFT-straight
- 8: For each sample in the SFT and RFT sets:
 - Convert sample format into instruction-following format with:
 - An image reference
 - A natural language prompt
 - A reasoning + answer pair
 - Append to respective output list (SFT or RFT)
- 9: Save both lists as JSON files

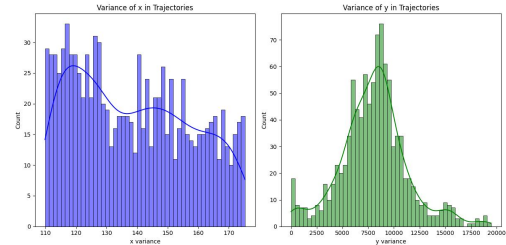


Figure 5. Distribution of trajectories in D_{easy} . trajectories exhibit lower x -variance than D_{hard} as can be seen in Fig. 6.

Each selected sample is then converted into an instruction-following format consisting of an image reference, a natural language prompt, and a corresponding reasoning-answer pair. These formatted samples are saved as separate JSON files for the SFT and RFT datasets.

B.2. Validation Set Construction

For evaluation, we construct validation sets focused on moderate and hard scenarios. We begin with a dense set of validation trajectories D_{dense} about 12K samples and remove any overlap with standard annotations $D_{standard}$ to ob-

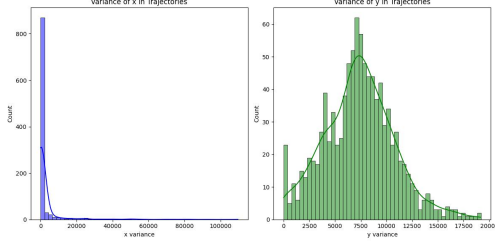


Figure 6. Distribution of trajectories in D_{hard} . trajectories exhibit lower x-variance than D_{easy} as can be seen in Fig. 5.

Table 9. Summary of Validation Subsets Construction

Subset	Sampling Strategy	#Trajectories
Easy (D_{easy})	Median-centered 1K slice of x -variance	1K
Hard (D_{hard})	0.7K from top 70% + 0.3K from bottom 10%	1K

tain candidate validation samples D_{val} . We compute the x -variance for each sample and sort them accordingly. To form the easy set D_{easy} , we select a middle slice (e.g., 1K samples centered around the median x -variance). For the hard set D_{hard} , we randomly sample 0.7K trajectories from the top 70% (high-variance) and 0.3K from the bottom 10% (low-variance) of the sorted list. Both validation subsets are saved as JSON files for downstream evaluation.

Algorithm 2 Construct Validation Sets (Easy, Hard)

- 1: Load dense validation trajectories D_{dense}
- 2: Load standard validation annotations $D_{standard}$
- 3: $D_{val} \leftarrow D_{dense} \setminus D_{standard}$
- 4: For each $d \in D_{val}$, compute variance of x over trajectory
- 5: $D_{sorted} \leftarrow \text{sort } D_{val} \text{ by } x\text{-variance (descending)}$
- 6: $N \leftarrow |D_{sorted}|$
- 7: **Easy Set:** $D_{easy} \leftarrow D_{sorted}[N/2 - 500 : N/2 + 500]$
- 8: **Hard Set:**
- 9: Randomly sample 700 from top 70% of D_{sorted}
- 10: Randomly sample 300 from bottom 10% of D_{sorted}
- 11: $D_{hard} \leftarrow \text{combined samples}$
- 12: Save D_{easy} and D_{hard} as JSON

References

[1] Jinze Bai, Shuai Bai, Shusheng Yang, Shijie Wang, Sinan Tan, Peng Wang, Junyang Lin, Chang Zhou, and Jingren Zhou. Qwen-vl: A versatile vision-language model for understanding, localization, text reading, and beyond. *arXiv preprint arXiv:2308.12966*, 2023. 1

[2] Kai Chen, Yanze Li, Wenhua Zhang, Yanxin Liu, Pengxiang Li, Ruiyuan Gao, Lanqing Hong, Meng Tian, Xinhai Zhao, Zhenguo Li, Dit-Yan Yeung, Huchuan Lu, and Xu Jia. Automated evaluation of large vision-language models on self-

driving corner cases. In *2025 IEEE/CVF Winter Conference on Applications of Computer Vision (WACV)*, pages 7817–7826, 2025. 4, 5

[3] Yanran Chen and Steffen Eger. Menli: Robust evaluation metrics from natural language inference. *Transactions of the Association for Computational Linguistics*, 11:804–825, 2023. 5

[4] Zhe Chen, Jiannan Wu, Wenhai Wang, Weijie Su, Guo Chen, Sen Xing, Muyan Zhong, Qinglong Zhang, Xizhou Zhu, Lewei Lu, Bin Li, Ping Luo, Tong Lu, Yu Qiao, and Jifeng Dai. Internvl: Scaling up vision foundation models and aligning for generic visual-linguistic tasks. In *Proceedings of the IEEE/CVF Conference on Computer Vision and Pattern Recognition (CVPR)*, pages 24185–24198, 2024. 1

[5] Tianzhe Chu, Yuexiang Zhai, Jihan Yang, Shengbang Tong, Saining Xie, Dale Schuurmans, Quoc V Le, Sergey Levine, and Yi Ma. Sft memorizes, rl generalizes: A comparative study of foundation model post-training. *arXiv preprint arXiv:2501.17161*, 2025. 2

[6] Haoyu Fu, Diankun Zhang, Zongchuang Zhao, Jianfeng Cui, Dingkan Liang, Chong Zhang, Dingyuan Zhang, Hongwei Xie, Bing Wang, and Xiang Bai. Orion: A holistic end-to-end autonomous driving framework by vision-language instructed action generation. *arXiv preprint arXiv:2503.19755*, 2025. 2

[7] Anurag Ghosh, Robert Tamburo, Shen Zheng, Juan R Alvarez-Padilla, Hailiang Zhu, Michael Cardei, Nicholas Dunn, Christoph Mertz, and Srinivasa G Narasimhan. Roadwork dataset: Learning to recognize, observe, analyze and drive through work zones. *arXiv preprint arXiv:2406.07661*, 2024. 4, 6

[8] Daya Guo, Dejian Yang, Haowei Zhang, Junxiao Song, Ruoyu Zhang, Runxin Xu, Qihao Zhu, Shirong Ma, Peiyi Wang, Xiao Bi, et al. Deepseek-r1: Incentivizing reasoning capability in llms via reinforcement learning. *arXiv preprint arXiv:2501.12948*, 2025. 2, 9

[9] Edward J Hu, Yelong Shen, Phillip Wallis, Zeyuan Allen-Zhu, Yuanzhi Li, Shean Wang, Lu Wang, Weizhu Chen, et al. Lora: Low-rank adaptation of large language models. *ICLR*, 1(2):3, 2022. 9

[10] Bo Jiang, Shaoyu Chen, Bencheng Liao, Xingyu Zhang, Wei Yin, Qian Zhang, Chang Huang, Wenyu Liu, and Xing-gang Wang. Senna: Bridging large vision-language models and end-to-end autonomous driving. *arXiv preprint arXiv:2410.22313*, 2024. 1, 2

[11] Bo Jiang, Shaoyu Chen, Qian Zhang, Wenyu Liu, and Xing-gang Wang. Alphadrive: Unleashing the power of vlms in autonomous driving via reinforcement learning and reasoning. *arXiv preprint arXiv:2503.07608*, 2025. 1, 2

[12] Bu Jin, Xinyu Liu, Yupeng Zheng, Pengfei Li, Hao Zhao, Tong Zhang, Yuhang Zheng, Guyue Zhou, and Jingjing Liu. Adapt: Action-aware driving caption transformer. In *2023 IEEE International Conference on Robotics and Automation (ICRA)*, pages 7554–7561. IEEE, 2023. 2

[13] Kimin Lee, Hao Liu, Moonkyung Ryu, Olivia Watkins, Yuqing Du, Craig Boutilier, Pieter Abbeel, Mohammad Ghavamzadeh, and Shixiang Shane Gu. Aligning text-

- to-image models using human feedback. *arXiv preprint arXiv:2302.12192*, 2023. 2
- [14] Kaican Li, Kai Chen, Haoyu Wang, Lanqing Hong, Chaoqiang Ye, Jianhua Han, Yukuai Chen, Wei Zhang, Chunjing Xu, Dit-Yan Yeung, et al. Coda: A real-world road corner case dataset for object detection in autonomous driving. In *European Conference on Computer Vision*, pages 406–423. Springer, 2022. 4
- [15] Haotian Liu, Chunyuan Li, Qingyang Wu, and Yong Jae Lee. Visual instruction tuning. In *Advances in Neural Information Processing Systems*, pages 34892–34916. Curran Associates, Inc., 2023. 1
- [16] Ziyu Liu, Zeyi Sun, Yuhang Zang, Xiaoyi Dong, Yuhang Cao, Haodong Duan, Dahua Lin, and Jiaqi Wang. Visual-rlft: Visual reinforcement fine-tuning. *arXiv preprint arXiv:2503.01785*, 2025. 2
- [17] Youssef Mroueh. Reinforcement learning with verifiable rewards: Grpo’s effective loss, dynamics, and success amplification. *arXiv preprint arXiv:2503.06639*, 2025. 2
- [18] Zhenghao Peng, Wenjie Luo, Yiren Lu, Tianyi Shen, Cole Gulino, Ari Seff, and Justin Fu. Improving agent behaviors with rl fine-tuning for autonomous driving. In *European Conference on Computer Vision*, pages 165–181. Springer, 2024. 2
- [19] Katrin Renz, Long Chen, Ana-Maria Marcu, Jan Hünemann, Benoit Hanotte, Alice Karnsund, Jamie Shotton, Elahe Arani, and Oleg Sinavski. Carllava: Vision language models for camera-only closed-loop driving. *arXiv preprint arXiv:2406.10165*, 2024. 2
- [20] Katrin Renz, Long Chen, Elahe Arani, and Oleg Sinavski. Simlingo: Vision-only closed-loop autonomous driving with language-action alignment. In *Proceedings of the Computer Vision and Pattern Recognition Conference*, pages 11993–12003, 2025. 2
- [21] John Schulman, Filip Wolski, Prafulla Dhariwal, Alec Radford, and Oleg Klimov. Proximal policy optimization algorithms. *arXiv preprint arXiv:1707.06347*, 2017. 3
- [22] Hao Shao, Yuxuan Hu, Letian Wang, Guanglu Song, Steven L. Waslander, Yu Liu, and Hongsheng Li. Lmdrive: Closed-loop end-to-end driving with large language models. In *Proceedings of the IEEE/CVF Conference on Computer Vision and Pattern Recognition (CVPR)*, pages 15120–15130, 2024. 2
- [23] Chonghao Sima, Katrin Renz, Kashyap Chitta, Li Chen, Hanxue Zhang, Chengen Xie, Jens Beißwenger, Ping Luo, Andreas Geiger, and Hongyang Li. Drivelm: Driving with graph visual question answering. In *Computer Vision – ECCV 2024*, pages 256–274, Cham, 2025. Springer Nature Switzerland. 2
- [24] Zirui Song, Guangxian Ouyang, Mingzhe Li, Yuheng Ji, Chenxi Wang, Zixiang Xu, Zeyu Zhang, Xiaoqing Zhang, Qian Jiang, Zhenhao Chen, et al. Maniplm-rl: Reinforcement learning for reasoning in embodied manipulation with large vision-language models. *arXiv preprint arXiv:2505.16517*, 2025. 2
- [25] Xiaoyu Tian, Junru Gu, Bailin Li, Yicheng Liu, Yang Wang, Zhiyong Zhao, Kun Zhan, Peng Jia, Xianpeng Lang, and Hang Zhao. Drivevlm: The convergence of autonomous driving and large vision-language models. *arXiv preprint arXiv:2402.12289*, 2024. 2
- [26] Milan Vojnovic and Se-Young Yun. What is the alignment objective of grpo? *arXiv preprint arXiv:2502.18548*, 2025. 2
- [27] Shihao Wang, Zhiding Yu, Xiaohui Jiang, Shiyi Lan, Min Shi, Nadine Chang, Jan Kautz, Ying Li, and Jose M Alvarez. Omnidrive: A holistic vision-language dataset for autonomous driving with counterfactual reasoning. In *Proceedings of the Computer Vision and Pattern Recognition Conference*, pages 22442–22452, 2025. 2
- [28] Jialong Wu, Shaofeng Yin, Ningya Feng, and Mingsheng Long. Rlv-world: Training world models with reinforcement learning. *arXiv preprint arXiv:2505.13934*, 2025. 2
- [29] Shaoyuan Xie, Lingdong Kong, Yuhao Dong, Chonghao Sima, Wenwei Zhang, Qi Alfred Chen, Ziwei Liu, and Liang Pan. Are vlms ready for autonomous driving? an empirical study from the reliability, data, and metric perspectives. *arXiv preprint arXiv:2501.04003*, 2025. 8
- [30] Zhenhua Xu, Yujia Zhang, Enze Xie, Zhen Zhao, Yong Guo, Kwan-Yee K Wong, Zhenguo Li, and Hengshuang Zhao. Drivegpt4: Interpretable end-to-end autonomous driving via large language model. *IEEE Robotics and Automation Letters*, 2024. 2
- [31] Zhenhua Xu, Yan Bai, Yujia Zhang, Zhuoling Li, Fei Xia, Kwan-Yee K Wong, Jianqiang Wang, and Hengshuang Zhao. Drivegpt4-v2: Harnessing large language model capabilities for enhanced closed-loop autonomous driving. In *Proceedings of the Computer Vision and Pattern Recognition Conference*, pages 17261–17270, 2025. 2
- [32] Jingyi Zhang, Jiaxing Huang, Huanjin Yao, Shunyu Liu, Xikun Zhang, Shijian Lu, and Dacheng Tao. R1-vl: Learning to reason with multimodal large language models via step-wise group relative policy optimization. *arXiv preprint arXiv:2503.12937*, 2025. 8
- [33] Tianyi Zhang, Varsha Kishore, Felix Wu, Kilian Q Weinberger, and Yoav Artzi. Bertscore: Evaluating text generation with bert. *arXiv preprint arXiv:1904.09675*, 2019. 5
- [34] Xingcheng Zhou, Xuyuan Han, Feng Yang, Yunpu Ma, and Alois C Knoll. Opendrivevla: Towards end-to-end autonomous driving with large vision language action model. *arXiv preprint arXiv:2503.23463*, 2025. 2